J. Fluid Mech. (2013), *vol.* 718, *pp.* 558–568.
doi:10.1017/jfm.2012.630

Fluid drainage from the edge of a porous reservoir

Zhong Zheng[1], Beatrice Soh[2], Herbert E. Huppert[3,4,5] and Howard A. Stone[1,†]

[1]Department of Mechanical and Aerospace Engineering, Princeton University, Princeton, NJ 08544, USA

[2]Department of Chemical and Biological Engineering, Princeton University, Princeton, NJ 08544, USA

[3]Institute of Theoretical Geophysics, Department of Applied Mathematics and Theoretical Physics, University of Cambridge, Wilberforce Road, Cambridge CB3 0WA, UK

[4]School of Mathematics, University of New South Wales, Kensington, NSW 2052, Australia

[5]Faculty of Science, University of Bristol, Bristol BS2 6BB, UK

(Received 7 August 2012; revised 15 November 2012; accepted 14 December 2012; first published online 8 February 2013)

We report theoretical and experimental studies to describe buoyancy-driven fluid drainage from a porous medium for configurations where the fluid drains from an edge. We first study homogeneous porous systems. To investigate the influence of heterogeneities, we consider the case where the permeability varies transverse to the flow direction, exemplified by a V-shaped Hele-Shaw cell. Finally, we analyse a model where both the permeability and the porosity vary transverse to the flow direction. In each case, a self-similar solution for the shape of these gravity currents is found and a power-law behaviour in time is derived for the mass remaining in the system. Laboratory experiments are conducted in homogeneous and V-shaped Hele-Shaw cells, and the measured profile shapes and the mass remaining in the cells agree well with our model predictions. Our study provides new insights into drainage processes such as may occur in a variety of natural and industrial activities, including the geological storage of carbon dioxide.

Key words: geophysical and geological flows, gravity currents

1. Introduction

Gravity currents propagating in porous media occur in a large variety of geophysical and industrial processes (Huppert 2006), including applications to CO_2 storage that have attracted much recent interest (Pacala & Socolow 2004; Metz *et al.* 2005; Zheng *et al.* 2010). Typically, the latter refers to injection of supercritical CO_2 into saline aquifers, where it is expected that, following injection, the lower-density CO_2 will migrate over more dense interstitial fluid. In many situations, these gravity-driven flows occur in long narrow geometries and can be described by similarity solutions (Gratton & Minotti 1990; Huppert & Woods 1995), including allowance for power-law injection scenarios (Huppert & Woods 1995; Lyle *et al.* 2005). Specific application of these ideas to CO_2 sequestration include a study of front propagation due to a constant injection rate in a confined porous medium (Nordbotten & Celia 2006*b*), analysis of

† Email address for correspondence: hastone@princeton.edu

the post-injection period (Hesse *et al.* 2007), and the influence of residual saturation and trapping (Hesse, Orr & Tchelepi 2008).

The above studies highlight the dynamics of spreading currents in homogeneous media over impermeable substrates. The effect of substrate permeability during the liquid injection process has been considered also. For example, the leakage from a gravity current flowing in a porous medium over a fractured substrate (Acton, Huppert & Worster 2001; Pritchard 2007; Hesse & Woods 2010), or a substrate with localized sinks (Neufeld *et al.* 2011), or line sinks (Vella *et al.* 2011) has been studied. In contrast, in this paper we focus on buoyancy-driven drainage from the edge of a porous reservoir, which is important when assessing long-term storage of buoyant materials such as CO_2 in a geological stratum. Previous studies related to this topic were mainly theoretical or numerical. For example, interface upconing around a well (Nordbotten & Celia 2006*a*) and the migration of a vertical gas plume through a heterogeneous porous medium (Silin, Patzek & Benson 2009) have been studied, where both of these examples were inspired, at least in part, by questions of CO_2 storage. We note that a similar problem of drainage from the water table, which can be treated as a gravity current, has also been studied theoretically, with strong assumptions being made on the boundary and initial conditions (e.g. Boussinesq 1904; Rupp & Selker 2005). In this paper, we will study the drainage problem theoretically, and verify the theoretical results using laboratory experiments in Hele-Shaw cells.

It is also important to understand the influence of heterogeneity on flow in porous media (e.g. Class & Ebigbo 2009). Pore-scale heterogeneity may induce unstable displacement processes when the capillary force is dominant, even with a mobility ratio that favours stability (Protiere *et al.* 2010). Macro-scale heterogeneities such as a gradient of the permeability could change the propagation behaviour of the front. For example, the influence of permeability variations in the flow direction are known to impact the imbibition process (Reyssat *et al.* 2009) and the interfacial stability in multi-phase displacement (Al-Housseiny, Tsai & Stone 2012). In this paper, we will examine the influence of permeability and porosity gradients perpendicular to the flow direction on the fluid drainage process driven by buoyancy.

In order to describe the fluid drainage behaviour from porous media, we examine the fundamental problem of drainage from an edge. We first present in § 2 a theoretical model of the problem and obtain a self-similar solution to the nonlinear partial differential equation (PDE) that describes the propagation. In § 3 we present the results of a series of laboratory experiments in a Hele-Shaw cell to compare with the theoretical results, and find good agreement. We study both the case of homogeneous porous media and the case with a vertical permeability gradient.

2. Theoretical study

We consider the problem of drainage of a viscous fluid from an edge of a model porous medium. In particular, we are interested in a buoyancy-driven gravity current in a porous system (figure 1*a*), where the fluid drains away by flowing over an edge (figure 1*b*), with x and y denoting the flow and transverse directions, respectively. We imagine fluid stored in a rectangular chamber of length L with an impermeable boundary at $x = 0$ and where the fluid drains at $x = L$. The unknown interface shape of the draining gravity current is denoted by $h(x, t)$. In the case of drainage from a uniform channel (figure 2*a*), we use the notation $h_c(x, t)$, and in the case of drainage from a V-shaped channel (figure 2*b*), which involves a spatially varying permeability, $k(y) = b^2(y)/12$, the shape is denoted by $h_v(x, t)$.

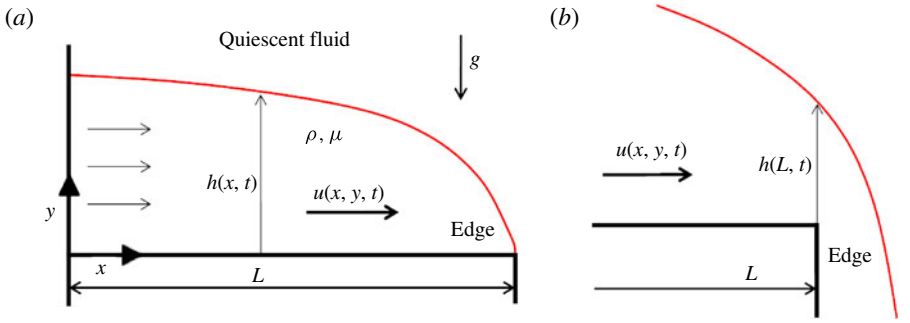

FIGURE 1. (Colour online) Sketch of a gravity current draining from the edge of a model porous medium. As emphasized in (*a*), the length of the current is constant. As shown in (*b*), near the edge, we assume that the height of the current $h(L, t) \to 0$, which corresponds to a late period of the drainage.

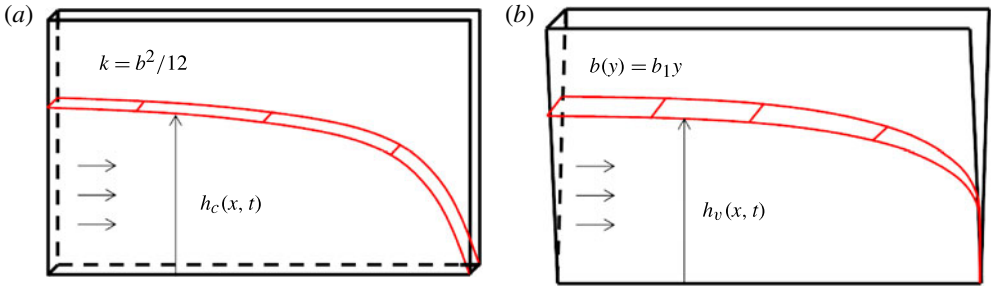

FIGURE 2. Sketch of the two Hele-Shaw cells we use to mimic the porous medium: (*a*) a uniform Hele-Shaw cell and (*b*) a V-shaped Hele-Shaw cell.

We make various approximations in this study. First, we assume that there is a sharp interface between the fluids (Bear 1972), which is expected to be a good approximation for a time scale shorter than those where diffusive effects cause variation transverse to the flow direction. Also, we neglect the influence of surface tension. The flow is driven by gravity acting on the density difference $\Delta\rho$ between the fluids. Second, when the gravity current is long and thin, we assume that the flow is nearly horizontal. This assumption is often called vertical equilibrium (Bear 1972; Yortsos 1995), since we take the pressure to be hydrostatic within the liquid. Third, we assume that drainage leads to the vanishing of the height of the profile near the edge, $h(L, t) \to 0$, i.e. the height at the edge is much smaller than the typical height of the gravity current (figure 1*b*). The adjustment period is relatively short, as confirmed by our experiments, and we concentrate on the long-time drainage problem because it is of primary concern. We refer to this later stage of the dynamics as the 'late period' of the drainage process, and we obtain similarity solutions for the time dependence of the drainage process. This solution does not satisfy the typical initial condition, but becomes a better and better model as time progresses. It should also be noted that, in the language of Barenblatt (1979), this solution is the intermediate asymptotic limit when the initial condition is not important.

A summary of the three analytical models we present is given in table 1. We discuss some of the details in the next three subsections.

2.1. *Uniform Hele-Shaw cell*

We begin by formulating the drainage problem for flow in a uniform Hele-Shaw cell, which models a homogeneous porous medium of permeability $k = b^2/12$, where b is the gap thickness. As is standard in studies of gravity currents, with the use of Darcy's law and the mass conservation equation, the shape of the current $h_c(x, t)$ is described by a nonlinear diffusion equation, derived for example by Boussinesq (1904), Huppert & Woods (1995) and others,

$$\frac{\partial h_c}{\partial t} = A_c \frac{\partial}{\partial x}\left(h_c \frac{\partial h_c}{\partial x}\right), \tag{2.1}$$

where $A_c = \Delta\rho g k/\mu$, g is gravity and μ is the viscosity of the liquid. Since the reservoir is sealed at $x = 0$, there is no horizontal flow there, i.e. $\partial h_c/\partial x = 0$. In the experiment, we have an initial condition $h_c(x, 0) = h_0$, though, as indicated above, we only consider times when the height at the draining edge ($x = L$) has approached zero. Therefore, we have two boundary conditions, which can be expressed as

$$\frac{\partial h_c}{\partial x}(0, t) = 0, \quad h_c(L, t) = 0. \tag{2.2a,b}$$

One difference with other gravity current problems is that here the horizontal length is a constant. Because the dimensions of A_c are length/time, and as the solution involves the variables $h_c(x, t, A_c, L)$, then dimensional analysis allows us to conclude that $h_c/L = f(x/L, A_c t/L)$. Second, the form of the PDE demands that $h_c \propto L^2/(A_c t)$, which, together with the results of dimensional analysis, suggests that the self-similar solution for (2.1) with boundary conditions (2.2) is given by

$$h_c(x, t) = \left(\frac{L^2}{A_c t}\right) f_c\left(\frac{x}{L}\right). \tag{2.3}$$

In this way, the nonlinear PDE is reduced to a nonlinear ordinary differential equation

$$(f_c f_c')' + f_c = 0, \quad f_c'(0) = 0, \quad f_c(1) = 0. \tag{2.4a,b,c}$$

This equation was solved numerically. The total liquid mass remaining in the porous medium is calculated according to

$$w_c(t) = \rho b \int_0^L h_c(x, t)\,\mathrm{d}x = \frac{\rho b L^3}{A_c t} \int_0^1 f_c(s)\,\mathrm{d}s. \tag{2.5a,b}$$

Consequently, we predict that the drainage has a power-law behaviour proportional to t^{-1}.

2.2. *V-shaped Hele-Shaw cell*

As a second study, we consider the gravity-driven drainage of fluid from an edge of a V-shaped Hele-Shaw cell (figure 2*b*), with the thickness of the cell at height y given by $b(y) = b_1 y$, where b_1 is a constant. The permeability is given by $k(y) = b^2(y)/12 = b_1^2 y^2/12$. Again, we assume that the fluid and the surroundings have a sharp interface between them and assume vertical equilibrium. An analysis of the gravity current accounting for this variation in permeability leads first to the

	Uniform Hele-Shaw cell	V-shaped Hele-Shaw cell	Porous media
Partial differential equations	$\dfrac{\partial h_c}{\partial t} = A_c \dfrac{\partial}{\partial x}\left(h_c \dfrac{\partial h_c}{\partial x}\right)$ $h_c(L, t) = 0$ $\dfrac{\partial h_c}{\partial x}(0, t) = 0$	$\dfrac{\partial h_v^2}{\partial t} = A_v \dfrac{\partial}{\partial x}\left(h_v^4 \dfrac{\partial h_v}{\partial x}\right)$ $h_v(L, t) = 0$ $\dfrac{\partial h_v}{\partial x}(0, t) = 0$	$\dfrac{\partial h^{m+1}}{\partial t} = A \dfrac{\partial}{\partial x}\left(h^{n+1} \dfrac{\partial h}{\partial x}\right)$ $h(L, t) = 0$ $\dfrac{\partial h}{\partial x}(0, t) = 0$
Solutions	$h_c(x, t) = \dfrac{L^2}{A_c t} f_c\left(\dfrac{x}{L}\right)$	$h_v(x, t) = \left(\dfrac{L^2}{A_v t}\right)^{1/3} f_c\left(\dfrac{x}{L}\right)$	$h(x, t) = \left(\dfrac{L^2}{At}\right)^{1/(n-m+1)} f\left(\dfrac{x}{L}\right)$
Ordinary differential equations	$(f_c f_c')' + f_c = 0$ $f_c(1) = 0$ $f_c'(0) = 0$	$(f_v^4 f_v')' + \dfrac{2}{3} f_v^2 = 0$ $f_v(1) = 0$ $f_v'(0) = 0$	$(f^{n+1} f')' + \dfrac{m+1}{n-m+1} f^{m+1} = 0$ $f(1) = 0$ $f'(0) = 0$
Mass in cell	$w_c(t) \approx t^{-1}$	$w_v(t) \approx t^{-2/3}$	$w(t) \approx t^{-(m+1)/(n-m+1)}$
Notes	$A_c = \dfrac{\Delta\rho g k}{\mu}$ $k = \dfrac{b^2}{12}$ b is a constant	$A_v = \dfrac{\Delta\rho g b_1^2}{24\mu}$ $k(y) = \dfrac{b_1^2 y^2}{12}$ $b(y) = b_1 y$	$A = \dfrac{\Delta\rho g k_1 (m+1)}{\mu \phi_1 (n+1)}$ $k(y) = k_1 y^n, \ \phi(y) = \phi_1 y^m$ $2 \leqslant \dfrac{n}{m} \leqslant 3$

TABLE 1. Summary of theoretical studies.

one-dimensional conservation law

$$\frac{\partial}{\partial t}\int_0^{h_v(x,t)} b(y)\,\mathrm{d}y + \frac{\partial}{\partial x}\int_0^{h_v(x,t)} b(y)u_v(x,y,t)\,\mathrm{d}y = 0, \tag{2.6}$$

where the flux is

$$u_v(x,y,t) = -\frac{k(y)}{\mu}\frac{\partial p(x,y,t)}{\partial x} = -\frac{k(y)\Delta\rho g}{\mu}\frac{\partial h_v(x,t)}{\partial x}. \tag{2.7a,b}$$

Therefore, we obtain a partial differential equation for the shape of the current $h_v(x,t)$ of the form

$$\frac{\partial h_v^2}{\partial t} = A_v\frac{\partial}{\partial x}\left(h_v^4\frac{\partial h_v}{\partial x}\right), \tag{2.8}$$

where $A_v = \Delta\rho g b_1^2/(24\mu)$, which is to be solved with boundary conditions

$$\frac{\partial h_v}{\partial x}(0,t) = 0, \quad h_v(L,t) = 0. \tag{2.9a,b}$$

Following the same techniques as described above, we find that a self-similar solution is given by

$$h_v(x,t) = \left(\frac{L^2}{A_v t}\right)^{1/3} f_v\left(\frac{x}{L}\right), \tag{2.10}$$

and the nonlinear partial differential equation is reduced to

$$(f_v^4 f_v')' + \tfrac{2}{3}f_v^2 = 0, \quad f_v'(0) = 0, \quad f_v(1) = 0. \tag{2.11a,b,c}$$

Again, the equation was solved numerically.

In this case, the liquid mass remaining in the Hele-Shaw cell is given by

$$w_v(t) = \frac{\rho b_1}{2}\int_0^L h_v^2(x,t)\,\mathrm{d}x = \frac{\rho b_1 L^{7/3}}{2A^{2/3}t^{2/3}}\int_0^1 f_v^2(s)\,\mathrm{d}s. \tag{2.12a,b}$$

Therefore, in particular, we predict theoretically that, when viscous fluid is draining from the edge of a V-shaped Hele-Shaw cell, the liquid mass remaining in the cell decreases in time with a power-law behaviour proportional to $t^{-2/3}$.

2.3. *Permeability and porosity gradients*

For a gravity current propagating in the x direction, we consider the more general case in which the porous medium has a vertical permeability gradient in the form $k(y) = k_1 y^n$, and a porosity gradient in the form $\phi(y) = \phi_1 y^m$, where k_1 and ϕ_1 are constants. However, m and n are generally not independent. In practice, it is found that $2 \leqslant n/m \leqslant 3$. In particular, $n/m = 2$ is representative of porous media with tubular fluid paths, and $n/m = 3$ is representative of porous media with an intersecting network of cracks or fissures as the fluid paths (Phillips 1991; Dullien 1992).

We again determine the time-dependent shape of the current, assuming a sharp interface between the two fluids, and neglect the vertical velocity. In this case, the one-dimensional conservation law is

$$\frac{\partial}{\partial t}\int_0^{h(x,t)} \phi(y)\,\mathrm{d}y + \frac{\partial}{\partial x}\int_0^{h(x,t)} u(x,y,t)\,\mathrm{d}y = 0, \tag{2.13}$$

where the flux is the same expression as in (2.7), i.e.

$$u(x, y, t) = -\frac{k(y)}{\mu}\frac{\partial p(x, y, t)}{\partial x} = -\frac{k(y)\Delta\rho g}{\mu}\frac{\partial h(x, t)}{\partial x}. \tag{2.14a,b}$$

Thus, the interface profile satisfies the nonlinear diffusion equation

$$\frac{\partial h^{m+1}}{\partial t} = A\frac{\partial}{\partial x}\left(h^{n+1}\frac{\partial h}{\partial x}\right), \tag{2.15}$$

where $A = \Delta\rho g k_1(m+1)/(\mu\phi_1(n+1))$, which is to be solved with boundary conditions

$$\frac{\partial h}{\partial x}(0, t) = 0, \quad h(L, t) = 0. \tag{2.16a,b}$$

This PDE has a self-similar solution of the form

$$h(x, t) = \left(\frac{L^2}{At}\right)^{1/(n-m+1)} f\left(\frac{x}{L}\right), \tag{2.17}$$

from which we find a nonlinear ordinary differential equation

$$(f^{n+1}f')' + \frac{m+1}{n-m+1}f^{m+1} = 0, \quad f'(0) = 0, \quad f(1) = 0. \tag{2.18a,b,c}$$

As above, we calculate the total liquid mass in the porous reservoir as

$$\begin{aligned} w(t) &= \frac{b\phi_1}{m+1}\int_0^L h^{m+1}(x, t)\,\mathrm{d}x \\ &= \frac{b\phi_1 L^{(n+m+3)/(n-m+1)}}{(m+1)A^{(m+1)/(n-m+1)}t^{(m+1)/(n-m+1)}}\int_0^1 f^{m+1}(s)\,\mathrm{d}s. \end{aligned} \tag{2.19a,b}$$

In the homogeneous case, we have $m = n = 0$, and the power-law behaviour reverts to t^{-1}, which agrees with (2.5). The special case in § 2.2 corresponds to $m = 1$, $n = 3$.

3. Experimental results

We conducted a series of drainage experiments in Hele-Shaw cells. Specifically, we first used a Hele-Shaw cell with a constant gap thickness to mimic a homogeneous porous medium (figure 2*a*) and then used a V-shaped cell with a constant gradient in gap thickness to mimic a porous medium with a permeability gradient transverse to the flow direction (figure 2*b*). The Hele-Shaw cells were made by joining two scratch-resistant clear cast acrylic sheets (McMaster-Carr, No. 8560K247). Glycerol–water solutions with different glycerol concentrations were used in the experiments, and the physical properties were determined from available tabulated results. To track the drainage, we placed the cell on a scale (Ohaus Scout Pro, SP4001), and recorded the mass in the cell as a function of time. We carried out experiments with various lengths and gap thicknesses of the Hele-Shaw cells. In a typical experiment, we filled the cell to a given height, removed a barrier on the side ($x = L$), which initiated drainage, and recorded the profile shape at different times using a USB camera. We then determined the fluid mass remaining in the cell, by subtracting the fluid drained from the total fluid mass in the cell at the beginning of the experiment.

3.1. *Uniform Hele-Shaw cell*

First, we present results for a uniform Hele-Shaw cell. Interface shapes at different times of a typical experiment are shown in figure 3. In this figure, we compare the

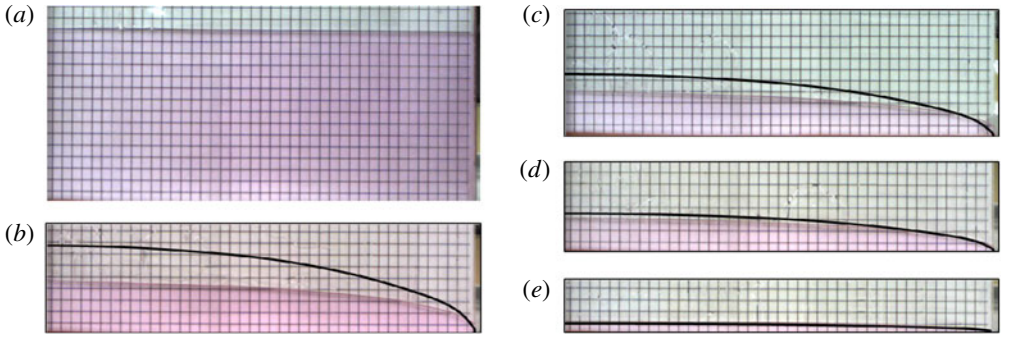

FIGURE 3. (Colour online) Images of a gravity current draining from a uniform Hele-Shaw cell, with comparisons between the experimental results and theoretical predictions (solid curve) for the shape, at various times: (*a*) $t = 0$ s; (*b*) $t = 250$ s; (*c*) $t = 350$ s; (*d*) $t = 500$ s; (*e*) $t = 2000$ s. In the late period, the self-similar solutions are seen to agree well with the experimental data. The liquid is pure glycerol, which is leaking from the right-hand edge of the cell. The grid has markings 1 cm apart.

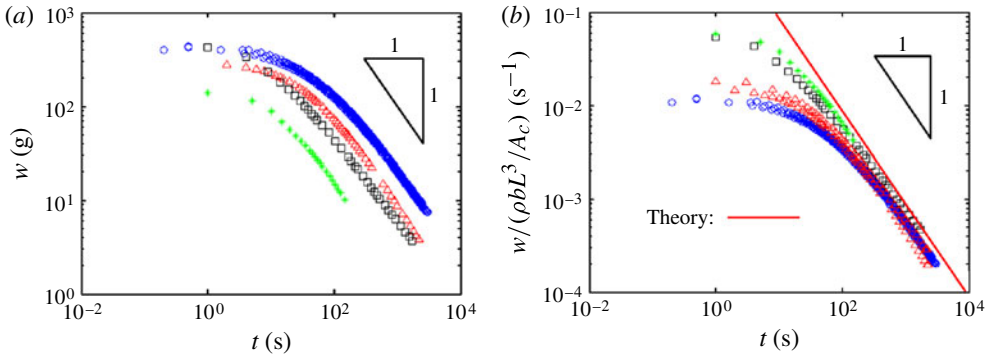

FIGURE 4. (Colour online) Comparison of the experimental results and the theoretical predictions for drainage from uniform Hele-Shaw cells. (*a*) Experimental results: liquid mass remaining in a Hele-Shaw cell versus time. (*b*) Re-scaled liquid mass versus time. The solid line is the prediction (2.5) from the theoretical study, with no fitting parameters. The typical value of gap thickness b in the experiments is 5 mm.

theoretical predictions of the profile shape (solid curve) with the experimental results, where all material and geometric parameters are measured so that there are no fitting parameters. As can be seen, after an initial period when $h(L, t)$ is finite (figure 3*a–c*), the predictions from the self-similar solution agree very well with the experimental results (figure 3*d*,*e*).

The liquid masses remaining in the cell for different experiments are plotted as functions of time in figure 4(*a*). We then rescale the experimental data of the liquid mass based on the theoretical study in § 2.1, and observe the collapse of data from different experiments (figure 4*b*). We also plot the prediction from the theoretical study as the solid curve in the figures. At longer times, the liquid mass exhibits a power-law behaviour t^{-1} as predicted. At early times, however, the experimental data were different from the model prediction. There are two reasons for the difference during

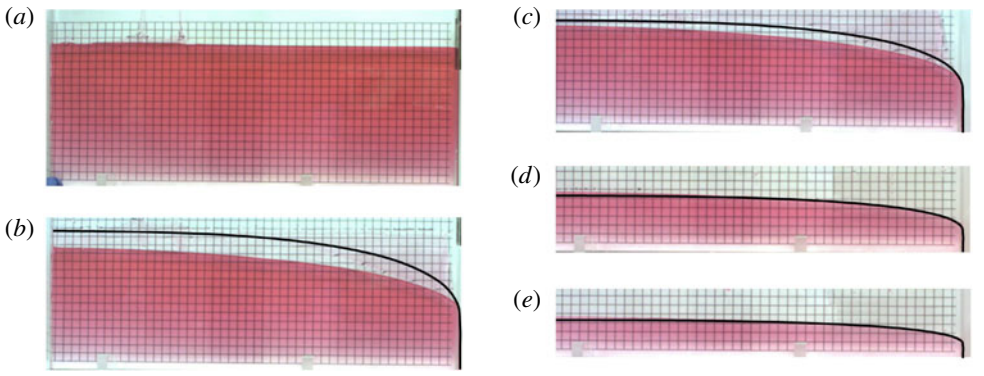

FIGURE 5. (Colour online) Images of a gravity current draining from a V-shaped Hele-Shaw cell, including comparisons of theoretical predictions and experimental results of the profile, at various times: (*a*) $t = 0$ s; (*b*) $t = 50$ s; (*c*) $t = 100$ s; (*d*) $t = 1000$ s; (*e*) $t = 3000$ s. The solid curve represents the predictions from the theoretical study. The liquid is pure glycerol, which is draining from the edge of the cell. The grid has markings 1 cm apart.

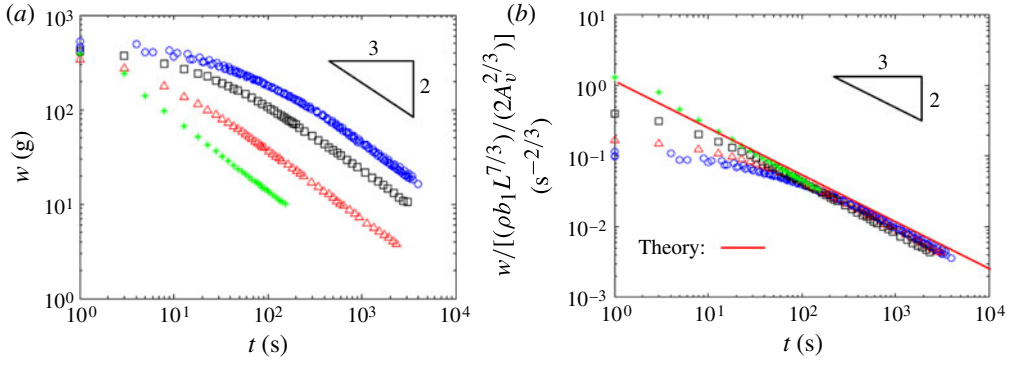

FIGURE 6. (Colour online) Experimental results on self-similar behaviour for fluid drainage from Hele-Shaw cells. (*a*) Liquid mass remaining in the Hele-Shaw cells versus time. (*b*) Re-scaled liquid mass in the Hele-Shaw cells versus time, based on (2.12), with no fitting parameters. The typical value of b_1 in the experiments is $\sim$0.05.

the early time period: (i) the initial conditions are still important at early times, and the long-time self-similar behaviour has not been obtained; (ii) the vertical velocity is not negligible, and therefore the horizontal flow assumption of the model fails during this period.

3.2. *V-shaped Hele-Shaw cell*

In order to study the influence of permeability variations and test the theoretical predictions, we conducted experiments in V-shaped Hele-Shaw cells (figure 2*b*). Typical results of the profile shapes are shown in figure 5, and are compared with the theoretical predictions (solid curves). Again, at early times we observe $h(L, t) \neq 0$, but, following an initial transition, the self-similar solutions give very good predictions.

The liquid masses in the cell versus time in different experiments are shown in figure 6(*a*). We also display the rescaled liquid weight as functions of time (figure 6*b*),

along with the theoretical predictions. In the late period, the liquid mass exhibited a power-law behaviour proportional to $t^{-2/3}$, as predicted by the theoretical study in § 2.2.

4. Summary and conclusions

In this paper, we first studied theoretically the problem of fluid drainage from an edge of a homogeneous porous medium. We also studied the drainage from an edge in the case where the permeability varies transverse to the flow direction (V-shaped Hele-Shaw cell), and a model where both the permeability and the porosity vary transverse to the flow direction. In all these cases, we found self-similar solutions for the drainage processes, and we predicted that the fluid mass remaining in the porous medium exhibits a power-law behaviour in time. Specifically, for the homogeneous porous medium, we found that the mass remaining in the medium is of the power-law behaviour t^{-1}; for the V-shaped Hele-Shaw cell, the power law is of the form $t^{-2/3}$; and finally, for the heterogeneous porous medium with both permeability and porosity variations given by $k(y) = k_1 y^n$ and $\phi(y) = \phi_1 y^m$, the remaining mass obeys a power-law behaviour of form $t^{-(m+1)/(n-m+1)}$.

To compare with the theoretical studies, we conducted laboratory experiments in uniform Hele-Shaw cells and V-shaped cells that have a constant vertical gradient in gap thickness. We recorded a series of profile shapes when the fluids drain from the cells. We also measured the fluid mass remaining in the cell when it drains. Following an initial adjustment period, we found that the experimental results agree well with theoretical predictions.

Understanding the buoyancy-driven drainage in porous materials can provide new insights into practical industrial processes such as geological CO_2 storage. In particular, after CO_2 has been injected into a porous reservoir, it is necessary to keep it underground for hundreds of thousands of years. However, in case there is a location where drainage can happen, such as produced by a poorly sealed well or a geological fault, because of buoyancy effects, CO_2 can drain and may possibly then leak into the atmosphere from underground. Our study predicts the time dependence of model fluid drainage processes from an edge, which is the extreme case when the vertical leakage pathway becomes infinitely permeable. It can help inform further engineering and regulatory studies focused on preventing unfavoured outcomes from CO_2 leakage, and so ensure CO_2 capture and storage as a reliable technology option for long-term climate mitigation.

Acknowledgements

We thank the Princeton Carbon Mitigation Initiative for support of this research. Also, we thank T. Al-Housseiny, T. Han, N. Lefevre-Marton, Z. Li, J. Neufeld, R. Socolow and J. Xia for helpful conversations. This research was conducted when H.E.H. was a visitor to the Mechanical and Aerospace Engineering Department, Princeton University. He particularly thanks the many members of the department for making his visit productive and enjoyable.

REFERENCES

ACTON, J. M., HUPPERT, H. E. & WORSTER, M. G. 2001 Two-dimensional viscous gravity currents flowing over a deep porous medium. *J. Fluid Mech.* **440**, 359–380.

AL-HOUSSEINY, T., TSAI, P. A. & STONE, H. A. 2012 Control of interfacial instabilities using flow geometry. *Nat. Phys.* **8**, 747–750.

BARENBLATT, G. I. 1979 *Similarity, Self-Similarity, and Intermediate Asymptotics*. Consultants Bureau.

BEAR, J. 1972 *Dynamics of Fluids in Porous Media*. Elsevier.

BOUSSINESQ, J. V. 1904 Recherches théorique sur l'écoulement des nappes d'eau infiltrées dans le sol et sur le débit des sources. *J. Math. Pures Appl.* **10**, 5–78.

CLASS, H. & EBIGBO, A. 2009 A benchmark study on problems related to CO_2 storage in geologic formations. *Comput. Geosci.* **13**, 409–434.

DULLIEN, F. A. 1992 *Porous Media: Fluid Transport and Pore Structure*. Academic Press.

GRATTON, J. & MINOTTI, F. 1990 Self-similar viscous gravity currents: phase plane formalism. *J. Fluid Mech.* **210**, 155–182.

HESSE, M. A., ORR, F. M. Jr & TCHELEPI, H. A. 2008 Gravity currents with residual trapping. *J. Fluid Mech.* **611**, 35–60.

HESSE, M. A., TCHELEPI, H. A., CANTWELL, B. J. & ORR, F. M. Jr 2007 Gravity currents in horizontal porous layers: transition from early to late self-similarity. *J. Fluid Mech.* **577**, 363–383.

HESSE, M. A. & WOODS, A. W. 2010 Buoyant disposal of CO_2 during geological storage. *Geophys. Res. Lett.* **37**, L01403.

HUPPERT, H. E. 2006 Gravity currents: a personal perspective. *J. Fluid Mech.* **554**, 299–322.

HUPPERT, H. E. & WOODS, A. W. 1995 Gravity driven flows in porous layers. *J. Fluid Mech.* **292**, 55–69.

LYLE, S., HUPPERT, H. E., HALLWORTH, M., BICKLE, M. & CHADWICK, A. 2005 Axisymmetric gravity currents in a porous medium. *J. Fluid Mech.* **543**, 293–302.

METZ, B., DAVIDSON, O., DE CONNICK, H., LOOS, M. & MEYER, L. 2005 *IPCC Special Report on Carbon Dioxide Capture and Storage*. Cambridge University Press.

NEUFELD, J. A., VELLA, D., HUPPERT, H. E. & LISTER, J. R. 2011 Leakage from gravity currents in a porous medium. Part 1. A localized sink. *J. Fluid Mech.* **666**, 391–413.

NORDBOTTEN, J. M. & CELIA, M. A. 2006*a* An improved analytical solution for interface upconing around a well. *Water Resour. Res.* **42**, W08433.

NORDBOTTEN, J. M. & CELIA, M. A. 2006*b* Similarity solutions for fluid injection into confined aquifers. *J. Fluid Mech.* **561**, 307–327.

PACALA, S. & SOCOLOW, R. 2004 Stabilization wedges: solving the climate problem for the next 50 years with current technologies. *Science* **305**, 968–972.

PHILLIPS, O. W. 1991 *Flow and Reactions in Porous Rocks*. Cambridge University Press.

PRITCHARD, D. 2007 Gravity currents over fractured substrates in a porous medium. *J. Fluid Mech.* **584**, 415–431.

PROTIERE, S., BAZANT, M. Z., WIETZ, D. A. & STONE, H. A. 2010 Droplet breakup in flow past an obstacle: a capillary instability due to permeability variations. *Europhys. Lett.* **92**, 54002.

REYSSAT, M., SANGNE, L. Y., VAN NIEROP, E. A. & STONE, H. A. 2009 Imbibition in layered systems of packed beads. *Europhys. Lett.* **86**, 56002.

RUPP, D. E. & SELKER, J. S. 2005 Drainage of a horizontal Boussinesq aquifer with a power law hydraulic conductivity profile. *Water Resour. Res.* **41**, W11422.

SILIN, D., PATZEK, T. W. & BENSON, S. M. 2009 A one-dimensional model of vertical gas plume migration through a heterogeneous porous medium. *Intl J. Greenh. Gas Control* **3**, 300–310.

VELLA, D., NEUFELD, J. A., HUPPERT, H. E. & LISTER, J. R. 2011 Leakage from gravity currents in a porous medium. Part 2. A line sink. *J. Fluid Mech.* **666**, 414–427.

YORTSOS, Y. C. 1995 A theoretical analysis of vertical flow equilibrium. *Trans. Porous Med.* **18**, 107–129.

ZHENG, Z., LARSON, E. D., LI, Z., LIU, G. & WILLIAMS, R. H. 2010 Near-term mega-scale CO_2 capture and storage demonstration opportunities in China. *Energy Environ. Sci.* **3**, 1153–1169.